The Astrophysical Journal Letters, 833:L29 (6pp), 2016 December 20 doi:10.3847/2041-8213/833/2/L29

REFINING THE DYNAMICAL CLOCK FOR STAR CLUSTERS

B. Lanzoni[1], F. R. Ferraro[1], E. Alessandrini[1], E. Dalessandro[2], E. Vesperini[3], and S. Raso[1]
[1] Department of Physics and Astronomy, University of Bologna, Viale Berti Pichat, 6/2, Bologna, Italy
[2] INAF Osservatorio Astronomico di Bologna, Via Ranzani 1, Bologna, Italy
[3] Department of Astronomy, Indiana University, Bloomington, IN 47401, USA
Received 2016 September 13; revised 2016 November 24; accepted 2016 November 29; published 2016 December 19

ABSTRACT

We used a sample of 25 Galactic globular clusters to empirically measure the parameter A^+ recently introduced by Alessandrini et al., and defined as the area enclosed between the cumulative radial distribution of blue straggler stars (BSSs) and that of a reference population. Based on *N*-body simulations, this parameter is expected to efficiently measure the level of BSS central segregation. Observationally, for a proper cluster-to-cluster comparison we use A^+_{rh}, i.e., the value of the parameter determined out to the half-mass radius in each system. We find that A^+_{rh} nicely correlates with the position of the minimum of the BSS normalized radial distribution and with the cluster central relaxation time. This demonstrates that it is a sensitive indicator of the cluster dynamical age as traced by the spatial segregation of the BSS population. In the context of the "stellar system dynamical clock," this parameter provides a new clock-hand, which is easier to determine observationally and allows a more robust measure of the cluster dynamical age.

Key words: globular clusters: general – methods: observational – stars: kinematics and dynamics

1. INTRODUCTION

Globular clusters (GCs) are dynamically active stellar systems, where the frequent gravitational interactions among stars, especially those involving binaries, significantly alter the overall energy budget, therefore leading to a variety of dynamical processes, as mass segregation, core collapse, etc. (e.g., Meylan & Heggie 1997). They also considerably affect the (otherwise normal) stellar evolution, generating exotic objects like blue straggler stars (BSSs), millisecond pulsars, X-ray binaries, and cataclysmic variables (e.g., Bailyn 1995) that cannot be explained by single-star evolutionary models. BSSs are the most abundant products of this activity. In the color–magnitude diagram they lie along an extrapolation of the main sequence (MS), brighter and bluer than the MS turnoff (e.g., Sandage 1953; Ferraro et al. 1993, 1997, 2004, 2006a; Lanzoni et al. 2007b, 2007a; Leigh et al. 2007; Dalessandro et al. 2008; Moretti et al. 2008; Beccari et al. 2011). Being more massive than normal cluster stars (Shara et al. 1997; Ferraro et al. 2006b; Fiorentino et al. 2014), BSSs are thought to be the result of two mass-enhancement processes: (1) mass-transfer in binary systems, possibly up to the complete coalescence of the two stars (McCrea 1964), and (2) stellar mergers due to direct collisions (Hills & Day 1976). The fraction of BSSs formed by either of the two mechanisms and its possible dependence on GC physical properties have been investigated in many recent works (e.g., Davies et al. 2004; Sollima et al. 2008; Chen & Han 2009; Ferraro et al. 2009; Knigge et al. 2009; Chatterjee et al. 2013a; Leigh et al. 2013; Sills et al. 2013; Xin et al. 2015), but they still need to be fully understood.

Independently of their formation mechanism, BSSs are recognized to be powerful probes of the dynamical history of GCs (e.g., Ferraro et al. 2009, 2015; Dalessandro et al. 2013b; Simunovic et al. 2014). The most convincing evidence has been recently provided by Ferraro et al. (2012, hereafter F12), who demonstrated that the observed shape of the BSS normalized radial distribution[4] (hereafter BSS-nRD) can be used as a *"dynamical clock"* able to measure the level of dynamical evolution reached by the system. In fact, old and chronologically coeval GCs can be separated in at least three distinct families on the basis of the shape of their BSS-nRD: Family I, where the distribution is flat (i.e., fully compatible with that of the light); Family II, where the BSS-nRD is bimodal (with a high peak in the cluster center, a dip at an intermediate radius $r_{\rm min}$, and a rising branch in the external regions); and Family III, where a central peak followed by a monotonically decreasing trend are observed. Since BSSs (and their binary progenitors) have masses larger than normal cluster stars, these behaviors have been interpreted as due to the progressive effect of dynamical friction, which drives the objects more massive than the average toward the cluster center, with an efficiency that decreases for increasing radial distance. Hence, a flat BSS-nRD indicates that dynamical friction has not played a major role yet in affecting the BSS population (not even in the innermost regions) and GCs belonging to Family I therefore are "dynamically young." In more evolved clusters (Family II), dynamical friction has been more and more efficient, affecting regions at increasingly larger distances from the center, as marked by the observed position of $r_{\rm min}$. In "dynamically old" systems, we expect that dynamical friction affected also the most remote BSSs, thus producing a monotonic BSS-nRD with a central peak only (as observed in Family III GCs).

The interpretation of the shape of the BSS-nRD as a probe of the host cluster dynamical age is also supported by several independent arguments. For instance, the class of dynamically old systems (Family III) includes M30, NGC 362, and M80, which are all clusters showing additional signatures (as a cuspy density profile) of their core-collapsing or core-collapsed stage (see Djorgovski & King 1986; Ferraro et al. 1999, 2009). Instead, the class of dynamically young clusters (Family I) includes ω Centauri (hereafter ω Cen), NGC 2419, Palomar 14, and NGC 6101, which are stellar systems with relaxation time comparable to their age. In the case of ω Cen and NGC 6101, the radial distribution of MS stars also reveals a level of mass segregation lower than what expected from equipartition

[4] With "normalized BSS distribution" here we indicate the double normalized ratio first introduced by Ferraro et al. (1993), defined as the ratio between the fraction of BSSs sampled in any adopted radial bin and the fraction of cluster light sampled in the same bin.

(Anderson 2002; Dalessandro et al. 2015), thus confirming their dynamically young state.

Dynamically intermediate-age clusters show a bimodal BSS-nRD with the position of the minimum varying as a function of the dynamical age: a tight relationship between the characteristic timescale of dynamical evolution of the system and the observed value of $r_{\rm min}$ expressed in units of the cluster core radius r_c has been found. Also in this case, additional independent observations confirm such a finding. In fact, whenever studied in comparable details, the radial distribution of binary systems has been found to be very similar to that of BSSs and to show the same value of $r_{\rm min}$ (Dalessandro et al. 2011; Beccari et al. 2013), in agreement with what is expected if they are both shaped by dynamical friction, as assumed in the dynamical clock framework. Along exactly the same line of reasoning, a different dynamical age for chronologically coeval clusters has been advocated to also explain the differing radial distributions of binary systems observed in two young and coeval clusters in the LMC (namely, NGC 1818 and NGC 1805, both having a chronological age of ∼30 Myr; Li et al. 2013). Indeed, detailed *N*-body modeling of these systems show that after a very early phase (just a few Myr from the formation) during which soft binaries are disrupted, a bimodal radial distribution of binaries develops and $r_{\rm min}$ progressively moves to larger values, until a unimodal distribution with only a central peak is found (see Figure 2 in Geller et al. 2013).

In spite of many, independent observational confirmations, the current generation of *N*-body and Monte Carlo simulations of GCs seems unable to reproduce the details of the BSS-nRD evolution, possibly indicating a still insufficient level of realism. In fact, while the peak of the distribution is seen to form in simulations, and the final stage of the synthetic BSS-nRD is indeed monotonic and single-peaked (Miocchi et al. 2015), a bimodal shape appears to be a temporary and unstable feature (see Miocchi et al. 2015; Hypki & Giersz 2016). This is at odds with the observations, which instead indicate that the BSS-nRD is bimodal in the vast majority of the investigated clusters (even in extragalactic environments; see the case of Hodge 11 discussed in Li et al. 2013). On the other hand, in cases of discrete and not numerous populations (as BSSs are) exactly locating the position of the minimum can be hard and somehow subjective.[5] Moreover, the correct identification of the minimum is critically dependent on the choice of the radial binning, since adopting too wide intervals tends to clean out the feature, while too narrow bins generate noisy distributions because of the decrease in the number of sampled BSSs. For this reason we started to search for other possible indicators of the BSS radial segregation process.

2. DEFINITION OF THE PARAMETER A^+

In Alessandrini et al. (2016), we used 10^5 particle *N*-body simulations to investigate the effect of dynamical friction on BSSs in GCs, and we studied the time evolution of a new parameter (A^+) providing a measure of the level of BSS segregation. The parameter is defined as the area enclosed between the cumulative radial distribution of BSSs, $\phi_{\rm BSS}(x)$, and that of a reference (lighter) population, $\phi_{\rm REF}(x)$:

$$A^+(x) = \int_{x_{\rm min}}^{x} \phi_{\rm BSS}(x') - \phi_{\rm REF}(x')\, dx', \quad (1)$$

where $x = \log(r/r_h)$ is the logarithm of the distance from the cluster center normalized to the half-mass radius r_h, and $x_{\rm min}$ is the minimum value sampled. Cluster-centric distances are expressed in logarithmic units to maximize the sensitivity of A^+ to the effects of dynamical friction (which is most efficient in the central cluster regions). Indeed, our *N*-body simulations demonstrate that this parameter increases significantly as a function of time, following the dynamical evolution of the cluster and, more specifically, tracking the process of segregation of BSSs relative to the reference population (see Figure 5 in Alessandrini et al. 2016). At initial times, when all stars are perfectly mixed regardless of their mass, BSSs and the REF population have the same cumulative radial distributions and $A^+ = 0$. As mass segregation proceeds, BSSs migrate toward the center of the system and the two curves start to separate, thus providing a progressively increasing value of the A^+ parameter. Alessandrini et al. (2016) also show that the rate of BSS segregation can be significantly slowed down by the presence of a population of stellar mass black holes, and this effect is clearly illustrated by differences in the time evolution of A^+.

3. OBSERVATIONAL DETERMINATION OF A^+

Given the theoretical results obtained from *N*-body simulations, it is now crucial to study this parameter also from the observational point of view. To empirically determine the value of A^+ in a significant number of GCs, we used the same photometric database from which the dynamical clock was defined (F12)[6], plus four additional clusters discussed in subsequent papers (Beccari et al. 2013; Dalessandro et al. 2013b; Sanna et al. 2014; Dalessandro et al. 2015). The details about the observations, data quality, and data analysis for each specific cluster can be found in those papers.

Here, we just provide a schematic summary of the data set characteristics and the general approach followed for the sample selection. The central regions of each cluster have been typically observed in the ultraviolet band with the Wide Field Planetary Camera 2 (WFPC2) on board the *Hubble Space Telescope* (*HST*), and, where possible, with complementary optical observations secured with the *HST* Advanced Camera for Surveys. The most external regions have been sampled by means of optical, ground-based observations performed with wide-field imagers, as the WFI@ESO and MegaCam@CFHT. Since BSSs are most reliably distinguishable from other cluster populations in the UV color–magnitude diagram (see Ferraro et al. 2015), we generally used this plane to define the BSS selection box. The latter is then transformed into the optical planes by using sub-samples of BSSs observed in both the UV and the optical bands. As reference populations, we generally considered red giant branch (RGB), sub-giant branch (SGB), and/or horizontal branch (HB) stars, depending on the cluster properties and the available photometric data. In order to allow unbiased comparisons, their selection was performed using the

[5] We estimate that, for thoughtful choices of the radial binning, the position of $r_{\rm min}$ can show variations of the order of ∼20%–25%, at most.

[6] For M10 here we adopt the quantities obtained in Dalessandro et al. (2013a).

same photometric catalogs adopted for the BSSs. However, depending on the surface temperature of each stellar population, we used the UV color–magnitude diagrams to select (hot) HB stars, and the optical planes for the (cool) RGB/SGB reference samples, so as to avoid any completeness bias. In the case of more than one reference population, we have verified that the corresponding radial distributions are in mutual agreement. This guarantees that any adopted reference population can be equivalently used for the determination of A^+.

By definition (see Section 2), A^+ depends on the considered cluster-centric distance. Hence, a meaningful cluster-to-cluster comparison requires that the parameter is measured over equivalent radial portions in every system and that the adopted region is large enough to be sensitive to the phenomenon that A^+ is describing (the effect of dynamical friction on BSSs). By using the set of *N*-body simulations discussed in Alessandrini et al. (2016), we verified that the value of the parameter computed at one half-mass radius is always representative of the cluster global value (i.e., the value attained if the entire radial extension is considered), corresponding to ∼70%–80% of it in all our runs. We also note that in the analysis of F12, the level of BSS sedimentation is parameterized by the value of $R_{\rm BSS}$: a central peak in the BSS-nRD corresponds to $R_{\rm BSS} > 1$, indicating that the observed number of BSSs is in excess with respect to what expected from the sampled luminosity. Interestingly, values of $R_{\rm BSS} > 1$ are observed at $r < r_h$ in all clusters belonging to Family II and Family III. This confirms that the region included within one half-mass radius is the most sensitive to the BSS sedimentation process. Thus, for a meaningful cluster-to-cluster comparison, in each system we determined the value of A^+ within one half-mass radius from the center[7] (hereafter A^+_{rh}). As expected, in the cases where two reference populations (HB and RGB/SGB) are available, the two resulting values of A^+_{rh} are very similar. We therefore adopted their mean value as the best estimate, and the standard deviation as their error. Since these latter range between 0.01 and 0.03, we attributed an error of 0.02 to all the cases where only one reference population is available. The values thus obtained are listed in Table 1, together with a few key parameters of the program clusters.

Table 1
Structural/Dynamical Parameters and Values of A^+_{rh} for the Program Clusters: Core Radius and Half-mass Radii in Arcseconds (Columns 2 and 3), Logarithm of the Central Relaxation Time in Gyr (Column 4), Value of $r_{\rm min}$ in Arcseconds (Column 5), Value of A^+_{rh} and Its Error (Columns 6 and 7)

Name	r_c	r_h	$\log(t_{rc})$	$r_{\rm min}$	A^+_{rh}	ϵ
ω Centauri	153.0	443.7	9.86	0.0	−0.010	0.010
Palomar 14	41.0	69.7	9.68	0.0	−0.010	0.010
NGC 6101	61.3	128.2	9.38	0.0	0.030	0.018
NGC 2419	20.0	54.0	10.08	0.0	0.035	0.007
NGC 5466	72.0	213.8	9.42	180.0	0.100	0.020
M55	99.0	215.8	9.00	405.0	0.100	0.020
M4	70.0	308.0	8.00	350.0	0.120	0.014
NGC 288	88.0	167.2	9.19	250.0	0.130	0.014
M53	26.0	98.8	9.08	55.0	0.150	0.014
M5	27.0	124.2	8.43	255.0	0.150	0.020
M10	41.0	139.8	8.26	425.0	0.160	0.000
M13	49.5	148.5	9.03	185.0	0.165	0.007
M2	17.0	57.8	8.48	150.0	0.170	0.028
NGC 6388	7.2	45.4	8.08	32.5	0.190	0.020
NGC 362	13.0	73.8	8.08	515.0	0.200	0.020
M79	9.7	47.5	7.98	325.0	0.250	0.020
M92	14.0	84.0	8.05	250.0	0.255	0.007
M3	30.0	186.0	8.75	125.0	0.260	0.020
NGC 5824	4.4	29.0	8.28	20.0	0.280	0.028
47 Tucanae	21.0	201.6	7.96	200.0	0.290	0.020
NGC 6229	9.5	30.4	8.72	25.0	0.290	0.000
M80	7.0	40.6	7.57	375.0	0.290	0.014
NGC 6752	13.7	194.5	7.37	325.0	0.325	0.021
M75	5.4	29.2	8.00	225.0	0.380	0.020
M30	4.3	109.2	6.79	385.0	0.520	0.000

Note. The values of the structural/dynamical parameters come from F12, Dalessandro et al. (2013a, 2013b), Beccari et al. (2013), Sanna et al. (2014), and Dalessandro et al. (2015). For NGC 6101 the value of $\log(t_{rc})$ has been recomputed by following Equation (10) in Djorgovski (1993) for homogeneity with the other clusters.

4. RESULTS AND DISCUSSION

Figure 1 (left panels) shows the cumulative radial distributions of BSSs and REF stars for four GCs in our sample. The labeled values of A^+_{rh} (see also Table 1) correspond to the size of the shaded areas: formally zero for ω Cen, which has a non-segregated BSS population (Family I cluster), and up to 0.52 for M30, which is one of the dynamically oldest system (Family III) in the sample, with BSSs much more centrally concentrated than the reference population. As listed in Table 1, the parameter is smaller than 0.05 also for the other three GCs with non-segregated BSS populations known so far, namely, Palomar 14, NGC 2419, and NGC 6101. In all the other cases, it assumes larger values, depending on the separation between the BSS and the reference star cumulative distributions. Qualitatively, this is exactly the behavior expected from a reliable indicator of BSS segregation. In the right panels of the figure we plot the radial distributions of the BSS double normalized ratio $R_{\rm BSS}$ for the same four clusters, with the black arrows indicating the position of the minimum $r_{\rm min}/r_c$. The figure clearly shows that the increases of A^+_{rh} seen from top to bottom in the left panels is accompanied by a systematic increase of $r_{\rm min}/r_c$ in the corresponding right panels, thus indicating that these two parameters are mutually linked, as expected if they describe the same phenomenon.

For a closer comparison with results of F12, we investigate the relation between A^+_{rh} and the parameter $\log(r_{\rm min}/r_c)$ for the entire sample of 25 GCs. We point out that, although both these quantities describe the progressive central segregation of BSSs, their definitions are completely independent and, in principle, they could be completely uncorrelated. Figure 2 shows, instead, that the two parameters are linked through a quite tight and direct correlation. Indeed, the Spearman rank correlation coefficient between A^+_{rh} and $r_{\rm min}/r_c$ is $\rho = 0.77$, corresponding to a probability $P > 99.99\%$ that the two parameters are correlated. The significance remains very high ($P > 99.7\%$) even if one (arbitrarily) excludes from the sample the most extreme points (namely, M30 and the four Family I GCs), or if limiting the analysis to the 13 clusters with the smallest errors on A^+_{rh} ($\epsilon < 0.02$). This confirms that A^+_{rh} and $r_{\rm min}/r_c$ are

[7] The available *HST* data are sufficient to cover such a region in almost all the selected clusters. Exceptions are M3, M4, and M55, for which complementary wide-field catalogs are also needed, and the clusters NGC 5466 and Palomar 14, which, by virtue of their low density, have been entirely sampled with ground-based observations (with LBC@LBT and MegaCam@CFHT, respectively; see Beccari et al. 2013, 2011). In the case of 47 Tucanae, only the WFPC2 data discussed in Ferraro et al. (2004) have been used.

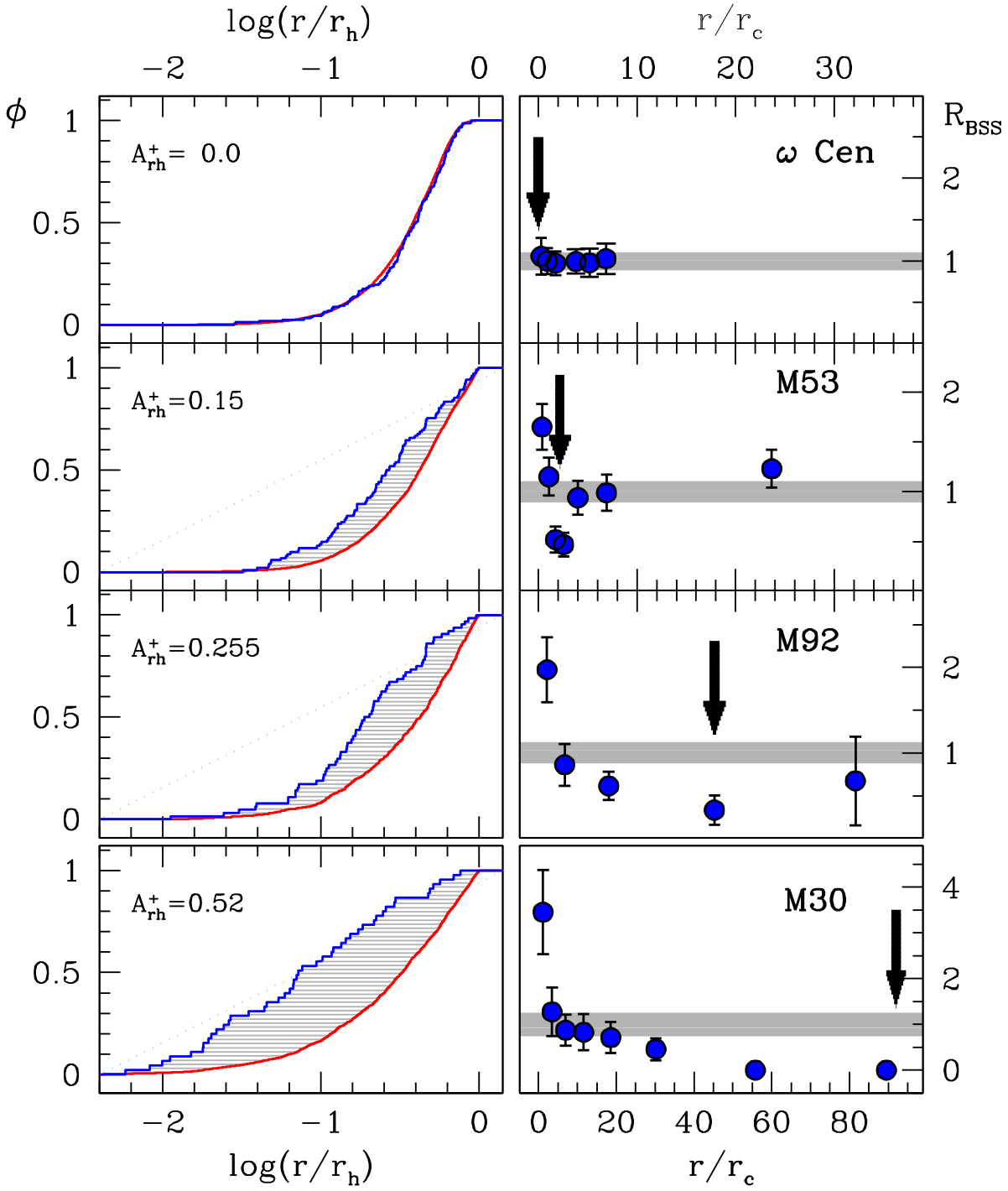

Figure 1. Left panels: cumulative radial distributions of BSSs (blue line) and REF stars (red line) observed within one half-mass radius (r_h) in four GCs of the considered sample (from top to bottom: ω Centauri, M53, M92, and M30). The size of the area between the two curves (shaded in gray) corresponds to the labeled value of A^+_{rh} (see also Table 1). Right panels: BSS normalized radial distribution ($R_{\rm BSS}$, blue circles) for the same clusters shown in the left panels. The black arrows mark the position of the BSS-nRD minimum ($r_{\rm min}/r_c$). The gray strips schematically show the distribution measured for the REF population.

actually different ways of measuring the same physical mechanism: as discussed in F12, the underlying process is dynamical friction, which, as clusters get dynamically older, progressively removes BSSs at increasingly larger distances from the center (thus generating a minimum at increasingly larger values of $r_{\rm min}/r_c$) and accumulates them toward the cluster center (thus increasing A^+_{rh}). As discussed in Alessandrini et al. (2016), the process of BSS segregation can be delayed by the presence of dark remnants and, in particular, by a population of stellar mass black holes. This adds another important element to the information contained in the BSS segregation level and the parameters introduced to measure it.

The results obtained suggest that A^+_{rh} could be used as an alternative indicator of the level of dynamical evolution experienced by star clusters since their formation, and we should expect that is related to other parameters measuring the

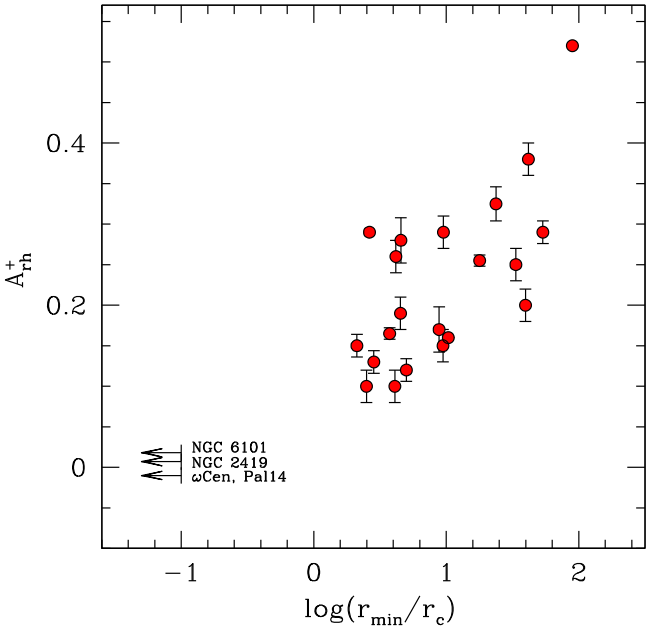

Figure 2. Parameter A^+_{rh} as a function of the observed position of the BSS-nRD minimum ($r_{\rm min}/r_c$) expressed in logarithmic units. For Family I clusters, with an everywhere flat BSS-nRD, a value $r_{\rm min}/r_c = 0.1$ has been arbitrarily assumed as an upper limit (see the arrows).

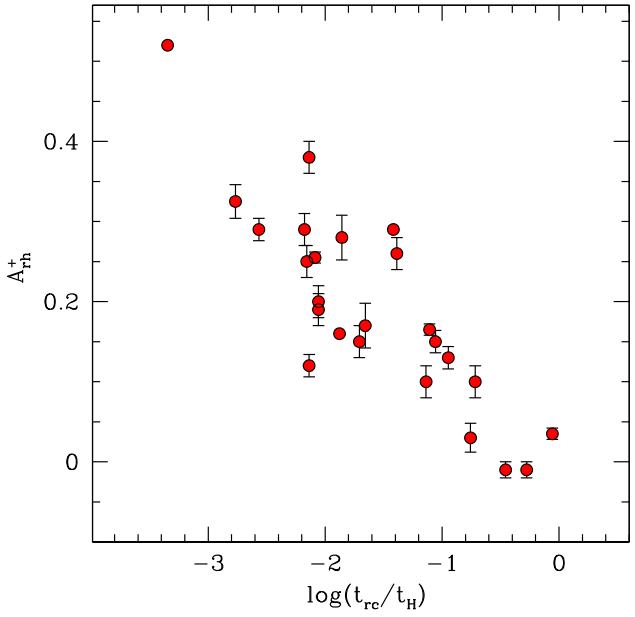

Figure 3. Relation between the new parameter A^+_{rh} and the logarithm of the cluster central relaxation time (t_{rc}) normalized to the Hubble time (t_H = 13.7 Gyr).

dynamical evolution timescale. Indeed, F12 found a nice correlation between the cluster-centric distance of the minimum of the BSS-nRD ($r_{\rm min}/r_c$) and the central relaxation time of the cluster (t_{rc}). Figure 3 shows that the latter is also tightly related to A^+_{rh}, in the sense that the proposed new parameter systematically decreases for increasing values of the relaxation time. The Spearman rank correlation coefficient between A^+_{rh} and t_{rc}/t_H (with $t_H = 13.7$ Gyr being the Hubble time) is $\rho = -0.81$, corresponding to $P > 99.99\%$, and it decreases only to $\rho = -0.63$ ($P = 99.7\%$) if Family I clusters and M30 are (arbitrarily) excluded from the sample. Also the Pearson correlation coefficient is very high ($r = -0.85$), indicating a strong linear correlation between A^+_{rh} and $\log(t_{rc}/t_H)$. As apparent from the figure, the relation between these two variables shows some scatter. This may indicate that further refinements should be used to measure A^+_{rh}, or, more likely, that the values of t_{rc} empirically estimated by following Djorgovski (1993) are rough approximations of the true relaxation times of Galactic GCs (as discussed, e.g., by Chatterjee et al. 2013b from dedicated Monte Carlo simulations). Besides the scatter, however, our analysis fully confirms that A^+_{rh} is a powerful indicator of cluster dynamical evolution and, once properly calibrated, it promises to be usable as an alternative, and hopefully more precise, measure of the central relaxation time of GCs.

In the framework of the dynamical clock originally defined by F12 in terms of the position of the minimum in the BSS-nRD ($r_{\rm min}/r_c$), the new parameter A^+ corresponds to a new clock-hand, while the engine of the clock remains the same (the dynamical friction process). From the observational point of view, the advantage of this new clock-hand is that it is easier to measure and somewhat less "fragile" than the position of the BSS-nRD minimum. In fact, for determining $r_{\rm min}$ it is necessary to sample the entire cluster radial extension (typically by means of a combination of *HST* and wide-field, ground-based observations), while only the central regions ($r < r_h$), possibly probed just by *HST*, are sufficient to measure A^+_{rh}. Moreover, it does not require any (somehow arbitrary) assumption on the radial binning (which is instead needed to build the BSS-nRD). Finally, from its own definition, $r_{\rm min}$ is located in a region of "low signal," where dynamical friction is removing heavy stars and the number of BSSs reaches its minimum (the so-called "zone of avoidance"; Mapelli et al. 2004, 2006); instead, A^+_{rh} is measured in a "high signal" region, where dynamical friction is accumulating heavy stars and the number of BSSs reaches its maximum. Thus, the proposed change of clock-hand makes the reading of the dynamical clock easier and less prone to low statistics uncertainties.

Realistic *N*-body simulations are now required to provide a calibration of A^+ as a function of the cluster dynamical age expressed in Gyr. It is important to emphasize that while this seems to be within the range of performances of the current generation of *N*-body simulations (see Alessandrini et al. 2016), a realistic calibration of the parameter requires simulations including virtually all the known ingredients (as dark remnants, primordial binaries, etc.).

We warmly thank the anonymous referee for useful comments that helped improve the presentation of the results. This research is part of the project Cosmic-Lab (see http://www.cosmic-lab.eu) funded by the European Research Council (under contract ERC-2010-AdG-267675).

REFERENCES

Alessandrini, E., Lanzoni, B., Miocchi, P., Ferraro, F. R., & Vesperini, E. 2016, ApJ, in press (arXiv:161004562A)
Anderson, J. 2002a, in ASP Conf. Ser. 265, Omega Centauri, A Unique Window into Astrophysics, ed. F. van Leeuwen, J. D. Hughes, & G. Piotto (San Francisco, CA: ASP), 87
Bailyn, C. D. 1995, ARA&A, 33, 133
Beccari, G., Dalessandro, E., Lanzoni, B., et al. 2013, ApJ, 776, 60

Beccari, G., Sollima, A., Ferraro, F. R., et al. 2011, ApJ, 737, 3
Chatterjee, S., Rasio, F. A., Sills, A., & Glebbeek, E. 2013a, ApJ, 777, 106
Chatterjee, S., Umbreit, S., Fregeau, J. M., & Rasio, F. A. 2013b, MNRAS, 429, 2881
Chen, X., & Han, Z. 2009, MNRAS, 395, 1822
Dalessandro, E., Ferraro, F. R., Lanzoni, B., et al. 2013a, ApJ, 770, 45
Dalessandro, E., Ferraro, F. R., Massari, D., et al. 2013b, ApJ, 778, 135
Dalessandro, E., Ferraro, F. R., Massari, D., et al. 2015, ApJ, 810, 40
Dalessandro, E., Lanzoni, B., Beccari, G., et al. 2011, ApJ, 743, 11
Dalessandro, E., Lanzoni, B., Ferraro, F. R., et al. 2008, ApJ, 681, 311
Davies, M. B., Piotto, G., & de Angeli, F. 2004, MNRAS, 349, 129
Djorgovski, S. 1993, in ASP Conf. Ser. 50, Structure and Dynamics of Globular Clusters, ed. S. G. Djorgovski & G. Meylan (San Francisco, CA: ASP), 373
Djorgovski, S., & King, I. R. 1986, ApJL, 305, L61
Ferraro, F. R., Beccari, G., Dalessandro, E., et al. 2009, Natur, 462, 1028
Ferraro, F. R., Beccari, G., Rood, R. T., et al. 2004, ApJ, 603, 127
Ferraro, F. R., Fusi Pecci, F., & Cacciari, C. 1993, AJ, 106, 2324
Ferraro, F. R., Lanzoni, B., Dalessandro, E., et al. 2012, Natur, 492, 393 (F12)
Ferraro, F. R., Lanzoni, B., Dalessandro, E., Mucciarelli, A., & Lovisi, L. 2015, in Ecology of Blue Straggler Stars, Astrophysics and Space Science Library, Vol. 413 (Berlin: Springer), 99
Ferraro, F. R., Paltrinieri, B., Fusi Pecci, F., et al. 1997, A&A, 324, 915
Ferraro, F. R., Paltrinieri, B., Rood, R. T., & Dorman, B. 1999, ApJ, 522, 983
Ferraro, F. R., Sabbi, E., Gratton, R., et al. 2006b, ApJL, 647, L53
Ferraro, F. R., Sollima, A., Rood, R. T., et al. 2006a, ApJ, 638, 433
Fiorentino, G., Lanzoni, B., Dalessandro, E., et al. 2014, ApJ, 783, 29
Geller, A. M., de Grijs, R., Li, C., & Hurley, J. R. 2013, ApJ, 779, 30
Hills, J. G., & Day, C. A. 1976, ApL, 17, 87
Hypki, A., & Giersz, M. 2016, MNRAS, submitted (arXiv:1604.07054)
Knigge, C., Leigh, N., & Sills, A. 2009, Natur, 457, 288
Lanzoni, B., Dalessandro, E., Ferraro, F. R., et al. 2007a, ApJ, 663, 267
Lanzoni, B., Sanna, N., Ferraro, F. R., et al. 2007b, ApJ, 663, 1040
Leigh, N., Knigge, C., Sills, A., et al. 2013, MNRAS, 428, 897
Leigh, N., Sills, A., & Knigge, C. 2007, ApJ, 661, 210
Li, C., de Grijs, R., & Deng, L. 2013, MNRAS, 436, 1497
Li, C., de Grijs, R., Deng, L., & Liu, X. 2013, ApJL, 770, L7
Mapelli, M., Sigurdsson, S., Colpi, M., et al. 2004, ApJL, 605, L29
Mapelli, M., Sigurdsson, S., Ferraro, F. R., et al. 2006, MNRAS, 373, 361
McCrea, W. H. 1964, MNRAS, 128, 147
Meylan, G., & Heggie, D. C. 1997, A&ARv, 8, 1
Miocchi, P., Pasquato, M., Lanzoni, B., et al. 2015, ApJ, 799, 44
Moretti, A., de Angeli, F., & Piotto, G. 2008, A&A, 483, 183
Sandage, A. R. 1953, AJ, 58, 61
Sanna, N., Dalessandro, E., Ferraro, F. R., et al. 2014, ApJ, 780, 90
Shara, M. M., Saffer, R. A., & Livio, M. 1997, ApJL, 489, L59
Sills, A., Glebbeek, E., Chatterjee, S., & Rasio, F. A. 2013, ApJ, 777, 105
Simunovic, M., Puzia, T. H., & Sills, A. 2014, ApJL, 795, L10
Sollima, A., Lanzoni, B., Beccari, G., Ferraro, F. R., & Fusi Pecci, F. 2008, A&A, 481, 701
Xin, Y., Ferraro, F. R., Lu, P., et al. 2015, ApJ, 801, 67